Eur. J. Mineral.
2006, **18**, 775-785

A structural, infrared, and Mössbauer spectral study of rosemaryite, $NaMnFe^{3+}Al(PO_4)_3$

FRÉDÉRIC HATERT[1,*], RAPHAËL P. HERMANN[2], ANDRÉ-MATHIEU FRANSOLET[1], GARY J. LONG[3] and FERNANDE GRANDJEAN[2]

[1]Laboratoire de Minéralogie, B18, Université de Liège, B-4000 Sart-Tilman, Belgium
[2]Département de Physique, B5, Université de Liège, B-4000 Sart-Tilman, Belgium
[3]Department of Chemistry, University of Missouri-Rolla, MO 65409-0010, USA

Abstract: Rosemaryite, ideally $NaMnFe^{3+}Al(PO_4)_3$, has been collected in the Buranga pegmatite, Rwanda. A single-crystal structure refinement was performed to $R_1 = 4.01$ %, in the $P2_1/n$ space group, with $a = 12.001(2)$, $b = 12.396(1)$, $c = 6.329(1)$ Å, $\beta = 114.48(1)°$, Vol. = 856.9(2) Å^3, $Z = 4$. The crystal structure and cation distributions are similar to those of ferrorosemaryite, $NaFe^{2+}Fe^{3+}Al(PO_4)_3$, and qingheiite, $Na_2MnMgAl(PO_4)_3$, but aluminium predominantly occurs in the M(2a) site, not in the M(2b) site as observed in ferrowyllieite, $Na_2Fe^{2+}{}_2Al(PO_4)_3$. The topologies of the X(1a) and X(1b) crystallographic sites are identical to those found in ferrorosemaryite, and correspond to a distorted octahedron and to a distorted cube, respectively. The [7+1]-coordinated X(2) site is a very distorted gable disphenoid, similar to the A(2)' site of the alluaudite structure. Mössbauer spectra have been obtained from 4.2 to 295 K, and fitted with a model including two Fe^{3+} and two Fe^{2+} doublets. The Fe^{2+} component corresponding to 2/3 of the Fe^{2+} spectral area and having a smaller quadrupole splitting of 2.63 mm/s at 15 K, is assigned to the Fe^{2+} on the M(2a) site, and the Fe^{2+} component with the larger quadrupole splitting of 3.17 mm/s at 15 K, is assigned to the Fe^{2+} on the M(1) site. Fe^{3+} is located only at the M(2a) and M(2b) sites, and the Fe^{3+} component corresponding to 3/4 of the Fe^{3+} and exhibiting the larger quadrupole spitting of 0.77 mm/s at 15 K, is most likely associated with Fe^{3+} on the M(2b) site. The infrared spectrum of rosemaryite shows absorption bands at 3450 and 1624 cm^{-1}, bands that arise from the vibrational modes of H_2O and confirm the presence of water in the channels of the wyllieite structure. A comparison of both the Mössbauer spectra and structural data of rosemaryite with those of other phosphates of the alluaudite and wyllieite groups, is also presented.

Key-words: Rosemaryite, phosphate mineral, structure refinement, Mössbauer spectroscopy, infrared spectroscopy.

Introduction

The wyllieite group of minerals consists of Na-Mn-Fe-Al-bearing phosphates which exhibit a crystal structure topologically similar to the alluaudite structure (Moore & Molin-Case, 1974). However, the ordering of cations in the wyllieite structure induces a splitting of the M(2) and X(1) sites of alluaudite into the M(2a) M(2b) and X(1a) X(1b) sites. Consequently, the $C2/c$ space group of alluaudite transforms into $P2_1/n$ in wyllieite with no concurrent change in the unit-cell parameters; the corresponding structural formula becomes X(2)X(1a)X(1b)M(1)M(2a)M(2b)$(PO_4)_3$ (Moore & Molin-Case, 1974).

In granitic pegmatites, particularly in the beryl-columbite-phosphate subtype of the rare-element pegmatites, according to the classification of Černý (1991), wyllieite-type phosphates display chemical compositions ranging from $Na_2(Mn,Fe^{2+})Fe^{2+}Al(PO_4)_3$ to $\square Na(Mn,Fe^{2+})Fe^{3+}Al(PO_4)_3$, with Ca^{2+} or Mn^{2+} replacing Na^+ on the X(2), X(1a) and X(1b) sites, Mg^{2+} or Zn^{2+} replacing iron on the M(2a) site, and Mg^{2+} or Fe^{3+} replacing Al^{3+} on the M(2b) site, where $\square$ represents a lattice vacancy (Moore & Ito, 1979). The crystal chemistry of these phosphates has been investigated by Moore & Ito (1979), who proposed a revision of their nomenclature based on chemical data. According to these authors, the name wyllieite corresponds to $Na_2MnFe^{2+}Al(PO_4)_3$, whereas the name rosemaryite designates the more oxidized compositions, such as $\square NaMnFe^{3+}Al(PO_4)_3$. The prefix ferro- is added if Fe^{2+} dominates in the M(1) site, thus leading to ferrowyllieite, $Na_2Fe^{2+}{}_2Al(PO_4)_3$ (Moore & Ito 1979). The name qingheiite has been introduced by Zhesheng *et al.* (1983) for the Mg-rich equivalent of wyllieite, $Na_2MnMgAl(PO_4)_3$.

More recently, the new mineral species ferrorosemaryite, $\square NaFe^{2+}Fe^{3+}Al(PO_4)_3$, has been described in the Rubindi pegmatite, Rwanda, and its crystal structure revealed that it belongs to the wyllieite group of minerals, with Al prevailing on the M(2a) site (Hatert *et al.*, 2005a).

*E-mail: fhatert@ulg.ac.be

0935-1221/06/0018-0775 $ 4.95
DOI: 10.1127/0935-1221/2006/0018-0775

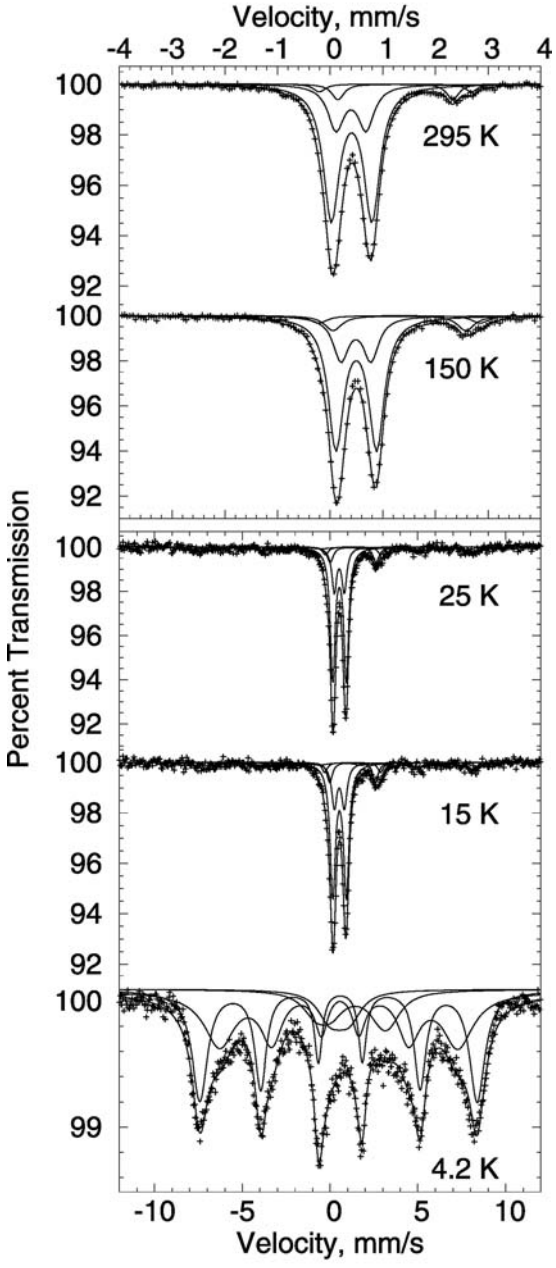

Fig. 1. Mössbauer spectra of rosemaryite from Buranga.

Table 1. Wet chemical analysis of rosemaryite from Buranga (Sample Bu 5.12; Fransolet, 1995).

	1	2
P_2O_5	44.18	3.000
Al_2O_3	8.30	0.785
Fe_2O_3	17.16	1.036
FeO	2.18	0.146
MnO	20.21	1.373
MgO	0.69	0.083
CaO	1.12	0.096
Na_2O	3.77	0.586
K_2O	0.03	0.003
H_2O^+	2.36	1.263
Total	100.00	

Analyst: J.-M. Speetjens. The analysis has been recalculated to 100%.

1. Weight %. 2. Number of cations calculated on the basis of 3 P per formula unit.

This unexpected cation distribution, different from that observed in ferrowyllieite by Moore & Molin-Case (1974), was the starting point of this new mineralogical investigation of rosemaryite, collected in the Buranga pegmatite and previously described by Fransolet (1995).

The aim of this study is to perform a single-crystal structure refinement on rosemaryite from Buranga, and to compare its structural data with those obtained for ferrowyllieite (Moore & Molin-Case, 1974), qingheiite (Zhesheng *et al*., 1983), ferrorosemaryite (Hatert *et al*., 2005a), and for the wyllieite-type compound $Na_{1.265}Mn^{2+}_{2.690}Mn^{3+}_{0.785}(PO_4)_3$, recently synthesized by Yakubovich *et al*. (2005). A Mössbauer spectral investigation of rosemaryite also permits a comparison with the Mössbauer spectrum of ferrorosemaryite (Hatert *et al*., 2005a), and with the spectra of more disordered alluaudite-type phosphates (Korzenski *et al*., 1998; Chouaibi *et al*., 2001; Hermann *et al*., 2002; Hatert *et al*., 2003, 2004 and 2005b; Hidouri *et al*., 2004; Redhammer *et al*., 2005).

Table 2. The hyperfine parameters obtained from the fits of the Mössbauer spectra between 15 and 295 K.

		Fe^{3+}					Fe^{2+}					Fe^{3+} magnetic phase			
Relative area[a]		**M(2a) 21.9%**		**M(2b) 65.6%**			**M(2a) 8.3%**		**M(1) 4.2%**						
Temperature	**Spectral area**	δ_{M2a}	$\Delta E_{Q,M2a}$	δ_{M2b}	$\Delta E_{Q,M2b}$	Γ	δ_{M2a}	$\Delta E_{Q,M2a}$	δ_{M1}	$\Delta E_{Q,M1}$	Γ	**Fe^{3+} fraction**	H	Γ	ΔE_Q
K	%ε.mm/s					mm/s						%	T		mm/s
295[a]	– 8.87	0.41	0.57*	0.40	0.77*	0.37	1.23	2.18	1.24	2.88	0.27	0	-	-	-
150	– 9.73	0.50	0.57*	0.49	0.77*	0.35	1.31	2.52	1.32	3.07	0.39	0	-	-	-
25	–11.21	0.53	0.57*	0.53	0.77*	0.33	1.36	2.62	1.38	3.15	0.44	17	47.6	1.2	–0.15
15	–11.11	0.53	0.57*	0.53	0.77*	0.37	1.36	2.63	1.38	3.17	0.43	18	47.7	1.0	–0.18
4.2	–12.3							–[b]							

[a]The Fe^{2+} has not been constrained for the 295 K spectrum and the fit yields 9.1%. The relative areas for the components are 68.2 and 22.7% for Fe^{3+} on M(2a) and M(2b), respectively, and 6.1 and 3 % for Fe^{2+} on M(2a) and M(1), respectively. For all other temperatures, including 4.2 K, the relative areas have been constrained.

[b]See table 3. * Parameter frozen during refinement.

Table 3. The hyperfine parameters obtained from the 4.2 K Mössbauer spectrum.

	% Area	*δ, mm/s*	*ΔE_Q, mm/s*	*H, T*	*Γ, mm/s*	*ΔΓ*	*θ, °*
Fe^{3+}	39(5)	0.534*	0.57*	42.4(7)	0.67(9)	0.21(3)	60(1)
Fe^{3+}	41(5)	0.534*	0.77*	48.9(1)	0.45(3)	0.08(1)	60(1)
Fe^{3+}	8(1)	0.534*	0*	4(1)	1.5(2)	0*	0*
Fe^{2+}	12.5*	1.38*	3.5(1)	4(2	1.7(3)	0*	97(1)

* Constrained parameter.

Table 4. Experimental details for the single-crystal X-ray diffraction study of rosemaryite from Buranga.

Dimensions of the crystal (mm)	*ca.* 0.17 × 0.32 × 0.07
a (Å)	12.001(2)
b (Å)	12.396(1)
c (Å)	6.329(1)
β (°)	114.48(1)
Space group	$P2_1/n$
Diffractometer	Bruker P4
Operating conditions	50 kV, 30 mA
Radiation	Mo$K\alpha$ (λ = 0.71073 Å)
Scan mode	ω scan
$2\theta_{max}$	60.8°
Range of indices	$-16 \le h \le 16$, $-1 \le k \le 17$, $-8 \le l \le 1$
Measured intensities	3510
Unique reflections	2493
Independent non-zero [$F_o > 4\sigma(F_o)$] reflections	2033
Absorption correction	Semi-empirical
Data reduction program	SHELXTL-Plus (Sheldrick, 1991)
Structure solution program	SHELXS97 (Sheldrick, 1997)
l.s. refinement program	SHELXL97 (Sheldrick, 1997)
Molecular graphics program	ATOMS (Dowty, 1993)
Refined parameters	193
R_1 (on *F*'s) ($F_o > 4\sigma(F_o)$)	0.040
R_1 (all)	0.053
wR_2 (all)	0.102
S (goodness of fit)	1.081
Max Δ/σ in the last l.s. cycle	0.000
Max peak and hole in the final ΔF map (e/Å^3)	+0.87 and –1.66

Experimental

Sample selection

The sample, Bu 5.12 from the Buranga pegmatite, Rwanda, investigated herein is the same as that described earlier by Fransolet (1995). The wet chemical analysis of this sample is given in Table 1. The unit-cell parameters, calculated from the X-ray powder diffraction pattern, are *a* = 11.977(2), *b* = 12.388(2), *c* = 6.320(1) Å, and *β* = 114.45(2)°. The primitive space group of rosemaryite from Buranga was confirmed by Fransolet (1995) from Weissenberg data.

Mössbauer spectroscopy

The iron-57 Mössbauer spectra of rosemaryite (Fig. 1) were recorded between 4.2 and 295 K on a constant acceleration spectrometer which used a rhodium matrix cobalt-57 source and was calibrated at 295 K with α-iron powder. The isomer shifts reported herein (Tables 2 and 3) are relative to α-iron at 295 K. The Mössbauer spectral absorber contained *ca*. 18 mg/cm^2 of powder.

Table 5. Final fractional coordinates and equivalent isotropic displacement parameters (Å^2) for rosemaryite from Buranga.

Site	**Atom**	***x***	***y***	***z***	U_{eq}
X(2)	Na*	–0.0002(5)	–0.0135(6)	0.246(1)	0.032(2)
X(1a)	Mn**	0.5	0	0	0.0442(5)
X(1b)	Na***	0.5	0	0.5	0.032(2)
M(1)	Mn****	0.00274(5)	–0.26107(5)	0.26214(9)	0.0108(2)
M(2a)	Al*****	0.27947(6)	–0.34053(6)	0.3605(1)	0.0071(2)
M(2b)	Fe******	0.22217(5)	–0.14821(4)	0.62934(9)	0.0075(2)
P(1)	P	0.00354(7)	–0.28313(7)	0.2413(1)	0.0077(2)
P(2a)	P	0.24199(7)	–0.09980(7)	0.1228(1)	0.0085(2)
P(2b)	P	0.24454(7)	0.11190(7)	0.6469(1)	0.0073(3)
O(1a)	O	0.4465(2)	–0.2854(2)	0.5177(4)	0.0111(5)
O(1b)	O	0.4523(2)	–0.7083(2)	0.0450(4)	0.0128(5)
O(2a)	O	0.1062(2)	–0.3509(2)	0.2250(4)	0.0170(5)
O(2b)	O	0.0884(2)	–0.6352(2)	0.7373(4)	0.0157(5)
O(3a)	O	0.3154(2)	–0.3299(2)	0.0893(4)	0.0115(5)
O(3b)	O	0.3340(3)	–0.6571(2)	0.6109(4)	0.0179(5)
O(4a)	O	0.1247(2)	0.4070(2)	0.3415(5)	0.0173(5)
O(4b)	O	0.1172(2)	–0.3999(2)	0.7738(4)	0.0129(5)
O(5a)	O	0.2336(2)	–0.1700(2)	0.3183(4)	0.0141(5)
O(5b)	O	0.2242(2)	–0.8170(2)	0.8299(4)	0.0118(5)
O(6a)	O	0.3114(2)	–0.4879(2)	0.3781(4)	0.0157(5)
O(6b)	O	0.3152(3)	–0.4975(2)	0.8740(5)	0.0199(6)

Refined sites occupancies:
*0.297(10) Na + 0.703(10) □; ****0.930(4) Mn + 0.070(4) □;
**0.487(3) Mn + 0.013(3) □; *****0.678(20) Al + 0.325(10) Fe;
***0.272(6) Na + 0.228(6) □; ******0.737(10) Fe + 0.267(20) Al.

Table 6. Selected bond distances (Å) and angles (°) for rosemaryite from Buranga.

P(1)-O(2a)	1.530(3)	X(2)-O(6a)	2.485(6)
P(1)-O(1b)	1.542(3)	X(2)-O(6b)'	2.515(6)
P(1)-O(2b)	1.545(3)	X(2)-O(6b)	2.659(7)
P(1)-O(1a)	1.545(2)	X(2)-O(1b)	2.697(8)
Mean	**1.541**	X(2)-O(6a)'	2.707(7)
		X(2)-O(3b)	2.785(7)
O(2a)-P(1)-O(1b)	113.3(1)	X(2)-O(1a)	2.819(8)
O(2a)-P(1)-O(2b)	105.7(2)	X(2)-O(3a)	3.045(8)
O(2a)-P(1)-O(1a)	107.7(1)	Mean	**2.714**
O(1b)-P(1)-O(2b)	108.4(1)		
O(1b)-P(1)-O(1a)	109.5(2)	X(1a)-O(4b) × 2	2.121(2)
O(2b)-P(1)-O(1a)	112.3(1)	X(1a)-O(2b) × 2	2.207(3)
Mean	**109.5**	X(1a)-O(4a) × 2	2.412(3)
		Mean	**2.247**
P(2a)-O(4a)	1.523(3)		
P(2a)-O(6a)	1.527(3)	X(1b)-O(2a) × 2	2.358(3)
P(2a)-O(5a)	1.550(3)	X(1b)-O(4a) × 2	2.359(3)
P(2a)-O(3b)	1.551(3)	X(1b)-O(4b) × 2	2.689(2)
Mean	**1.538**	X(1b)-O(2b) × 2	2.856(3)
		Mean	**2.566**
O(4a)-P(2a)-O(6a)	111.3(2)		
O(4a)-P(2a)-O(5a)	109.0(1)	M(1)-O(1a)	2.176(2)
O(4a)-P(2a)-O(3b)	109.5(2)	M(1)-O(4b)	2.194(3)
O(6a)-P(2a)-O(5a)	110.3(2)	M(1)-O(1b)	2.213(3)
O(6a)-P(2a)-O(3b)	109.4(1)	M(1)-O(4a)	2.249(3)
O(5a)-P(2a)-O(3b)	107.3(1)	M(1)-O(3b)	2.252(3)
Mean	**109.5**	M(1)-O(3a)	2.284(3)
		Mean	**2.228**
P(2b)-O(6b)	1.514(3)		
P(2b)-O(4b)	1.529(3)	M(2a)-O(6a)	1.860(3)
P(2b)-O(3a)	1.543(2)	M(2a)-O(2a)	1.897(3)
P(2b)-O(5b)	1.553(3)	M(2a)-O(3a)	1.940(3)
Mean	**1.535**	M(2a)-O(1a)	1.955(2)
		M(2a)-O(5b)	2.000(3)
O(6b)-P(2b)-O(4b)	110.7(2)	M(2a)-O(5a)	2.173(3)
O(6b)-P(2b)-O(3a)	108.7(1)	Mean	**1.971**
O(6b)-P(2b)-O(5b)	111.0(2)		
O(4b)-P(2b)-O(3a)	111.7(1)	M(2b)-O(6b)	1.920(3)
O(4b)-P(2b)-O(5b)	107.1(1)	M(2b)-O(3b)	2.022(3)
O(3a)-P(2b)-O(5b)	107.6(1)	M(2b)-O(5a)	2.047(3)
Mean	**109.5**	M(2b)-O(1b)	2.060(3)
		M(2b)-O(2b)	2.077(3)
		M(2b)-O(5b)	2.172(3)
		Mean	**2.050**

Infrared spectroscopy

The infrared spectrum of rosemaryite (Fig. 2) was recorded with a Nicolet NEXUS spectrometer, from 32 scans with a 1 cm^{-1} resolution, between 400 and 4000 cm^{-1}. The sample was prepared by thoroughly mixing 2 mg of sample with KBr in order to obtain a 150 mg homogeneous pellet which was subsequently dried for several hours at 120°C. To prevent water contamination, the measurements were performed under a dry air purge.

Structure refinement

The X-ray structural study was carried out on a Bruker P4 four-circle diffractometer (MoK_α radiation, $\lambda = 0.71073$ Å), on a crystal fragment of 0.17 × 0.32 × 0.07 mm. The unit-cell parameters and standard deviations were calculated for the setting angles of 37 reflections with $9.8° < 2\theta < 24.9°$: $a = 12.001(2)$, $b = 12.396(1)$, $c = 6.329(1)$ Å, and $\beta = 114.48(1)°$. The intensities of 3510 reflections, corresponding to 2493 unique reflections ($R_{int.} = 0.037$), were measured by the ω scan technique in the range $3.3° < 2\theta < 60.8°$ ($h = \bar{16} \rightarrow 16$, $k = \bar{1} \rightarrow 17$, $l = \bar{8} \rightarrow 1$). Data were corrected for Lorentz polarization and absorption effects, the latter with a semi-empirical method using a reliable set of ψ-scan data (North *et al.*, 1968).

The crystal structure was refined in space group $P2_1/n$, which was confirmed from systematic absences. The starting atomic coordinates were those of ferrowyllieite (Moore & Molin-Case, 1974), and scattering curves for neutral atoms, together with anomalous dispersion corrections, were taken from *International Tables for X-ray Crystallography, Vol. C* (Wilson, 1992). Cation occupancies were refined to obtain better agreement with the chemical composition of rosemaryite (Table 1). For simplicity, Ca^{2+} and Mg^{2+}, which are present in very low amounts, were not taken into account in the crystal structure refinement. Finally, the relative occupancies of Fe^{3+} and Al^{3+} on the M(2a) and M(2b) sites, of Mn^{2+} and vacancies on the X(1a) and M(1) sites, and of Na^{+} and vacancies on the X(2) and X(1b) sites, were refined. The refinement was completed using anisotropic displacement parameters for all atoms. The final conventional R_1 factor was 0.040. Further details of the intensity data collection and refinement are given in Table 4.

Final positional and isotropic thermal parameters for rosemaryite are given in Table 5, and selected bond distances and angles are given in Table 6. Anisotropic thermal parameters are available from the authors or through the EJM editorial office – Paris.

Mössbauer spectroscopy

Model

The general appearance of the Mössbauer spectra obtained between 15 and 295 K indicates that they should be fit with at least two doublets, one with a small isomer shift and quadrupole splitting assigned to Fe^{3+}, and one with a large isomer shift and quadrupole splitting assigned to Fe^{2+} (Fig. 1). However, both the poor fits and the broad lines obtained from preliminary fits reveal that an acceptable fit will require at least two Fe^{3+} doublets and two Fe^{2+} doublets. Such four doublet fits, with no constraints on the hyperfine parameters, indicate both that the 12.5 % Fe^{2+} fraction is essentially independent of temperature below 150 K and that the quadrupole splittings of both Fe^{3+}

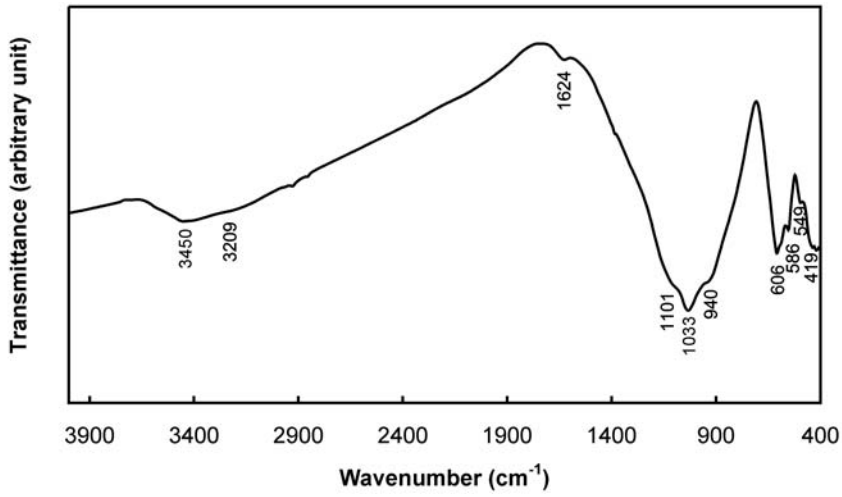

Fig. 2. Infrared spectrum of rosemaryite from Buranga.

Table 7. Refined site populations (RSP, *apfu*), refined site-scattering values (RSS, *epfu*), mean bond-lengths (MBL, Å), assigned site populations (ASP, *apfu*), calculated site-scattering values (CSS, *epfu*), and calculated bond lengths (CBL, Å) for rosemaryite from Buranga.

	Results of the structure determination			**Results of the chemical analysis**		
Site	**RSP**	**RSS**	**MBL**	**ASP**	**CSS**	**CBL***
X(2)	0.297 Na	3.3	2.667**	0.436 Na^{+}	4.8	2.600
X(1a)	0.487 Mn	12.2	2.247	0.450 Mn^{2+} + 0.050 Na^{+}	11.8	2.249
X(1b)	0.272 Na	3.0	2.566	0.100 Na^{+} + 0.069 Mn^{2+}	2.8	2.510
M(1)	0.930 Mn	23.3	2.228	0.754 Mn^{2+} + 0.096 Ca^{2+} + 0.083 Mg^{2+} + 0.067 Fe^{2+}	23.5	2.234
M(2a)	0.678 Al + 0.325 Fe	17.3	1.971	0.685 Al^{3+} + 0.236 Fe^{3+} + 0.079 Fe^{2+}	17.1	1.980
M(2b)	0.737 Fe + 0.267 Al	22.6	2.050	0.800 Fe^{3+} + 0.100 Al^{3+} + 0.100 Mn^{2+}	24.6	2.053

*: The CBL values have been calculated from the ASP, assuming a full occupancy of the crystallographic sites.
**: For the calculation of the X(2)-O MBL, the very long X(2)-O(3a) bond has not been taken into account.

Table 8. Bond-valence table (vu) for rosemaryite from Buranga.

	X(2)	**X(1a)**	**X(1b)**	**M(1)**	**M(2a)**	**M(2b)**	**P(1)**	**P(2a)**	**P(2b)**	**Σ**
O(1a)	0.064			0.357	0.479		1.215			2.12
O(1b)	0.089			0.323		0.434	1.225			2.07
O(2a)			0.220 *		0.561		1.265			2.05
O(2b)		0.325 *	0.057 *			0.415	1.215			2.01
O(3a)	0.035			0.267	0.499				1.221	2.02
O(3b)	0.070			0.291		0.481		1.195		2.04
O(4a)		0.187 *	0.219 *	0.293				1.289		1.99
O(4b)		0.410 *	0.090 *	0.340					1.269	2.11
O(5a)					0.266	0.450		1.199		1.92
O(5b)					0.425	0.321			1.189	1.94
O(6a)	0.245				0.620			1.275		2.14
O(6b)	0.245					0.634			1.321	2.20
$S_{calc.}$	0.75	1.84	1.17	1.87	2.85	2.73	4.92	4.96	5.00	
$S_{theor.}$	1.00	1.90	1.41	2.00	2.92	2.90	5.00	5.00	5.00	

The bond valences were calculated from the bond lengths given in Table 6, and from the assigned site populations of Table 7, with the parameters of Brown & Altermatt (1985). *: Bond valences were multiplied by two, for the calculation of the valence on the X(1a) and X(1b) crystallographic sites. A full occupancy has been assumed for the X(2) and X(1b) sites.

components are temperature independent within their error limits. Further, essentially temperature independent ratios of 2:1 and 3:1 were observed for the areas of the two Fe^{3+} and two Fe^{2+} components, respectively. Thus for the final fits, the Fe^{2+} content has been constrained to 12.5 % of the total iron and, for the Fe^{3+} doublets, constrained quadrupole

splittings of 0.772 and 0.571 mm/s have been used for the components with relative areas of 1/3 and 2/3, respectively. In contrast, for the Fe^{2+} doublets, constrained relative areas of 1/4 and 3/4 have been used for the components with the small and large quadrupole splittings, respectively. At 15 and 25 K a weak magnetic sextet is observed with a hyperfine field of ~ 48 T; the area of this sextet must be added to the Fe^{3+} fraction in order to ensure a constant Fe^{2+} content at low temperature.

The final fit of the 150 K spectrum involved the adjustment of 10 parameters, four isomer shifts, δ, two Fe^{2+} quadrupole splittings, ΔE_Q, two line widths, Γ, one each for the Fe^{2+} and Fe^{3+} components, as well as the total spectral area and spectral baseline. In addition, for the 295 K spectrum, the Fe^{2+} content has been varied and, for the 15 and 25 K spectra, four additional parameters, the area, the hyperfine field, the quadrupole interaction, and the line width of the broad sextet, have been varied. The isomer shift of this sextet was constrained to 0.53 mm/s, the average of the Fe^{3+} isomer shifts at higher temperature.

The Mössbauer spectrum measured at 4.2 K indicates the presence of long range magnetic hyperfine interactions. The relatively large absorption at –6 and +6.5 mm/s indicates the presence of two different contributions, with rather large magnetic hyperfine fields that can be assigned to Fe^{3+}. Because the absorption at 2.5 mm/s is much smaller at 4.2 than at 15 K, the Fe^{2+} components associated with the absorption at this velocity at 15 K must also be magnetically split at 4.2 K, although with a smaller hyperfine magnetic field. Because the Fe^{2+} quadrupole and magnetic hyperfine interactions are similar, a fit of the 4.2 K spectrum requires the diagonalization of the Hamiltonian. Thus the fit has used a three magnetic component model with one Fe^{2+} and two Fe^{3+} sextets plus an additional small Fe^{3+} component, with a large line width and a small hyperfine field. The latter component is required to fit the incomplete magnetic ordering at 4.2 K. A comparison with other spectra obtained for alluaudites indicate that the 4.2 K spectrum of rosemaryite is similar to the incompletely ordered alluaudite spectrum of natural $NaMnFe_2(PO_4)_3$ obtained at 15 K (Hatert *et al.*, 2004). Apparently complete magnetic ordering in rosemaryite occurs below 4.2 K. Except for the 12.5 % Fe^{2+} content, the relative spectral absorption areas of the spectral components have not been constrained to those of the paramagnetic spectra. The isomer shifts obtained at 15 K have been used at 4.2 K in order to reduce the number of free parameters; the quadrupole interactions observed at 15 K have been constrained for the two Fe^{3+} magnetic components and allowed to vary for the Fe^{2+} component; the resulting value was consistent with the higher temperature values. Unfortunately, field distributions prevent the attribution of the magnetic components to a specific site. Further, an incremental broadening parameter, $\Delta\Gamma$, was introduced for the two Fe^{3+} components in order to mimic a distribution of the hyperfine fields that results from variations in the local environment; the line width at a given velocity, v, relative to the isomer shift, δ, of a component is then given by $\Gamma + \Delta\Gamma \cdot \mathrm{abs}(v - \delta)$. The hyperfine parameters obtained from the final fits are given in Tables 2 and 3.

Site assignment

The iron ions in rosemaryite are located on three M(1), M(2a), and M(2b) sites. A possible assignment of the two Fe^{3+} and the two Fe^{2+} components to specific sites can be obtained through a comparison with an earlier Mössbauer spectral study of ferrorosemaryite (Hatert *et al.*, 2005a). In ferrorosemaryite, Fe^{2+} is located on the M(1) and M(2a) sites and the quadrupole splitting of ~3.3 mm/s for the Fe^{2+} on the M(1) site is much larger than the splitting of ~2.3 mm/s for the Fe^{2+} on the M(2a) site. In rosemaryite, it is thus reasonable to attribute the Fe^{2+} component that corresponds to 2/3 of the Fe^{2+} spectral area and has the smaller quadrupole splitting of 2.63 mm/s at 15 K, to Fe^{2+} on the M(2a) site, and the Fe^{2+} component with the larger quadrupole splitting of 3.17 mm/s at 15 K, to Fe^{2+} on the M(1) site. In ferrorosemaryite, Fe^{3+} is located on three sites and the more distorted M(1) site corresponds to the larger quadrupole splitting of 1.03 mm/s. Because no Fe^{3+} component with such a large quadrupole splitting is observed in the rosemaryite Mössbauer spectra, Fe^{3+} is most likely found only on the M(2a) and M(2b) sites. In ferrorosemaryite, the M(2b) site accommodates most of the Fe^{3+} and corresponds to the larger quadrupole splitting of ~0.74 mm/s; in rosemaryite, the Fe^{3+} component with the larger spectral area, 3/4 of the Fe^{3+}, also exhibits the larger quadrupole spitting, and can most likely be assigned to Fe^{3+} on the M(2b) site. The hyperfine parameters of the smaller area component, 1/4 of the Fe^{3+}, are close to those observed for Fe^{3+} on M(2a) in ferrorosemaryite in which δ is 0.51 mm/s and ΔE_Q is 0.52 mm/s at 85 K and, thus, the assignment of the smaller area component to Fe^{3+} on M(2a) seems reasonable.

The incremental broadening discussed above and shown in Fig. 1 is not unreasonable because the variety of the near-neighbour environments on the M(2a) and M(2b) sites will yield a distribution of hyperfine fields. However, the relative areas of the spectral lines of the magnetic sextets have been constrained to the usual 3:2:1:1:2:3 ratio. Because of the distribution of cations on the different sites, the hyperfine parameters obtained on the Fe^{2+} are less reliable but do provide an indication of the magnitude of the correct hyperfine interactions (Table 3).

Infrared spectroscopy

The infrared spectrum of rosemaryite (Fig. 2) is similar to those of alluaudite-type phosphates (Antenucci *et al.*, 1993; Hatert *et al.*, 2002, 2003, 2005b) and of ferrorosemaryite (Hatert *et al.*, 2005a), with stretching vibrational modes of the PO_4 tetrahedra in the 1200 to 850 cm^{-1} region, PO_4 bending vibrational modes between *ca*. 400 and 650 cm^{-1}, and lattice vibrations at lower frequencies.

It is important to note the large absorption band found at 3450 cm^{-1} (Fig. 2), a band that is related to the O–H stretching vibrational mode (Farmer, 1974). The presence of protons in natural alluaudites has been suspected by Fransolet *et al.* (1994) on the basis of wet chemical analyses, and the synthetic protonated alluaudite-type

compounds $M^{+}M^{2+}_3(PO_4)(HPO_4)_2$, where M^{+} is Na^{+} or Ag^{+} and M^{2+} is Mn^{2+} or Co^{2+}, have been synthesized by Lii & Shih (1994), Leroux *et al*. (1995a and b) and Guesmi & Driss (2002). More recently, single-crystal X-ray diffraction and infrared spectroscopic investigations of the new arsenate mineral, yazganite, $NaFe^{3+}_2(Mg,Mn)(AsO_4)_3\cdot H_2O$, have demonstrated the existence of molecular water localized in channel 2 of the alluaudite structure, at position 0.003(1), 0.0004(4), 0.272(2) (Sarp & Černý, 2005).

The rosemaryite infrared absorption band at 1624 cm^{-1} (Fig. 2), is assigned to the bending vibrational mode of H_2O, and its observation confirms the presence of molecular water in the channels of the wyllieite structure. According to the wet chemical analysis (Table 1), the H_2O content of rosemaryite from Buranga reaches 0.63 molecules per formula unit, and the formula of this mineral corresponds to $(\square_{0.88}Na_{0.12})(Na_{0.47}Ca_{0.10}Mn_{0.43})(Mn_{0.94}Fe^{2+}_{0.06})(Fe^{3+}_{0.83}Fe^{2+}_{0.09}Mg_{0.08})(Al_{0.79}Fe^{3+}_{0.21})(PO_4)_3\cdot 0.63H_2O$. In the infrared spectrum of ferrorosemaryite (Hatert *et al*., 2005a), an absorption band was observed at 3375 cm^{-1}, but without any absorption band around 1600 cm^{-1}. Consequently, these authors tentatively assigned the band at 3375 cm^{-1} to the stretching vibrations of OH^{-} groups localised at the apex of an HPO_4^{2-} tetrahedron, but this assignment probably should be revised in view of the better quality of the infrared data obtained for rosemaryite.

Structure refinement

The basic features of the rosemaryite structure are identical to those of the other members of the wyllieite group (Moore & Molin-Case, 1974; Zhesheng *et al*., 1983; Yakubovich *et al*., 2005; Hatert *et al*., 2005a). The structure consists of kinked chains of edge-sharing octahedra stacked parallel to {101}. These chains are formed by a succession of M(2a)–M(2b) octahedral pairs, linked by highly distorted M(1) octahedra. Equivalent chains are connected in the *b* direction by the P(1), P(2a), and P(2b) phosphate tetrahedra to form sheets oriented perpendicular to [010]. These interconnected sheets produce channels parallel to *c*, channels that contain the large X sites.

A detailed cationic distribution has also been established, by taking into account the results of the chemical analyses, of the Mössbauer spectral study, and of the single-crystal structure refinement. The results given in Table 7 indicate that the refined site populations (RSP), obtained from the single-crystal structure refinement (Table 5), are in good agreement with the assigned site populations (ASP), deduced from the chemical and Mössbauer spectral results. Moreover, the refined site scattering values (RSS) and the mean bond lengths (MBL), obtained from the structure refinement, are very close to the calculated site scattering values (CSS) and the calculated bond lengths (CBL), respectively (Table 7). This agreement confirms the reliability of the assigned site populations.

The bond valence table for ferrorosemaryite is given in Table 8, where the bond valence sums were calculated as $s = \exp[(R_0 - R)/0.37]$, by using the R_0 values of Brown & Altermatt (1985). The bond valences for oxygen are close to the theoretical value of 2.00, and the bond valences for phosphorus are very close to the theoretical value of 5.00 (Table 8). For all the cationic sites, a good correspondence between the theoretical and the calculated valence values is generally observed.

Finally, bond length distortion (BLD) and bond angle distortion (BAD) parameters were calculated for the *M* sites of the rosemaryite structure, with a method modified from Renner & Lehmann (1986) and already used by Hatert *et al.* (2004). The distortion parameters are much higher for the M(1) site (BLD = 1.51; BAD = 14.28) than for M(2a) (BLD = 0.40; BAD = 7.38) and M(2b) (BLD = 0.31; BAD = 9.85), thus confirming the site assignments proposed for the interpretation of the Mössbauer spectra (see above).

Discussion

The crystal structure and cation distribution of wyllieite-type phosphates

In addition to an unpublished diploma thesis (Brier, 2000), only three crystal structure refinements on wyllieite-type minerals have been reported, one for ferrowyllieite (Moore & Molin-Case, 1974), a second for qingheiite (Zhesheng *et al*., 1983), and a third for ferrorosemaryite (Hatert *et al*., 2005a). The mean *M*–O bond lengths and the cation distributions among the different crystallographic sites of these minerals are given in Table 9, and compared with the data obtained by Yakubovich *et al*. (2005) on the synthetic wyllieite-type compound, $Na_{1.265}Mn^{2+}_{2.690}Mn^{3+}_{0.785}(PO_4)_3$.

A careful examination of the atomic coordinates reported by Zhesheng *et al*. (1983) indicate that the M(2a)-M(2b) and X(1a)-X(1b) pairs of crystallographic sites, which result from a splitting of the M(2) and X(1) sites of the alluaudite structure, have been inverted in qingheiite. Atomic coordinates similar to those given by Moore & Molin-Case (1974) can be obtained by applying the translation $x, y - 0.5, z - 0.5$. For consistency, the names used for the crystallographic sites of qingheiite by Zhesheng *et al*. (1983) have been inverted in Table 9 and in the following discussion.

Compared to ferrowyllieite and qingheiite, ferrorosemaryite and rosemaryite are highly oxidized, and consequently contain a significant number of vacancies per formula unit. For this reason, in ferrorosemaryite, the X(2) site is unoccupied, and the X(1b) site contains 0.310(4) vacancies per formula unit (Hatert *et al*., 2005a). In rosemaryite, the X(2) site contains 0.703(10) vacancies per formula unit, whereas X(1a) and X(1b) contain 0.013(3) and 0.228(6) vacancies per formula unit, respectively (Table 5).

The X(1a) site of rosemaryite is shown in Fig. 3a, and corresponds to a very distorted octahedron, while the X(1b) site (Fig. 3b) can be described as a very distorted cube. The topologies of these sites are identical to those described in qingheiite and ferrorosemaryite (Zhesheng *et*

Table 9. Comparison of the unit-cell parameters, assigned site populations (ASP, *apfu*), and mean bond lengths (MBL, Å) for wyllieite-type phosphates.

		Ferrowyllieite	Ferrorosemaryite	Rosemaryite	Qingheiite	Synthetic compound
References		1	2	3	4	5
Ideal formula		$Na_2Fe^{2+}{}_2Al(PO_4)_3$	$\square NaFe^{2+}Fe^{3+}Al(PO_4)_3$	$\square NaMn^{2+}Fe^{3+}Al(PO_4)_3$	$Na_2MnMgAl(PO_4)_3$	$Na_2Mn^{2+}{}_2Mn^{3+}(PO_4)_3$
Space group		$P2_1/n$	$P2_1/n$	$P2_1/n$	$P2_1/n$	$P2_1/c$
***a* (Å)**		11.868(15)	11.838(1)	12.001(2)	11.856(3)	6.5291(6)
***b* (Å)**		12.382(12)	12.347(1)	12.396(1)	12.411(3)	12.653(1)
***c* (Å)**		6.354(9)	6.2973(6)	6.329(1)	6.421(1)	10.952(1)
β (°)		114.52(8)	114.353(6)	114.48(1)	114.45(2)	97.18(1)
M(2a)	**ASP**	$1.00Fe^{2+}$	$0.72Al^{3+} + 0.14Fe^{2+} + 0.14Fe^{3+}$	$0.69Al^{3+} + 0.24Fe^{3+} + 0.08Fe^{2+}$	$0.42Al^{3+} + 0.26Fe^{2+} + 0.18Mg^{2+} + 0.13Fe^{3+} + 0.01Zn^{2+}$	$1.00Mn^{2+}$
	MBL	2.098	1.963	1.971	2.001	2.164
M(2b)	**ASP**	$0.75Al^{3+} + 0.25Fe^{2+}$	$0.88Fe^{3+} + 0.10Al^{3+} + 0.02Mg$	$0.80Fe^{3+} + 0.10Al^{3+} + 0.10Mn^{2+}$	$0.95Mg^{2+} + 0.05Mn^{2+}$	$0.79Mn^{3+} + 0.21Mn^{2+}$
	MBL	1.973	2.019	2.050	2.092	2.046
M(1)	**ASP**	$0.75Fe^{2+} + 0.25Mg^{2+}$	$0.57Fe^{2+} + 0.20Fe^{3+} + 0.18Na^{+} + 0.05Mn^{2+}$	$0.75Mn^{2+} + 0.10Ca^{2+} + 0.08Mg^{2+} + 0.07Fe^{2+}$	$1.00Mn^{2+}$	$1.00Mn^{2+}$
	MBL	2.225	2.175	2.228	2.221	2.235
X(1a)	**ASP**	$0.46Na^{+} + 0.04\ \square$	$0.43Mn^{2+} + 0.07Na^{+}$	$0.45Mn^{2+} + 0.05Na^{+}$	$0.50Mn^{2+}$	$0.41Na^{+} + 0.09\ \square$
	MBL	2.533	2.255	2.247	2.242	2.602
X(1b)	**ASP**	$0.25Ca^{2+} + 0.25Mn^{2+}$	$0.17Na^{+} + 0.04Mn^{2+} + 0.04Ca^{2+} + 0.25\ \square$	$0.10Na^{+} + 0.07Mn^{2+} + 0.33\ \square$	$0.50Na^{+}$	$0.48Mn^{2+} + 0.02\ \square$
	MBL	2.209	2.543	2.566	2.541	2.279
X(2)	**ASP**	$0.70Na^{+} + 0.30\ \square$	$1.0\ \square$	$0.44Na^{+} + 0.56\ \square$	$0.81Na^{+} + 0.08Ca^{2+} + 0.11\square$	$0.85Na^{+} + 0.15\ \square$
	MBL	2.723	-	2.667	2.732	2.635

1. Moore & Molin-Case (1974); 2. Hatert *et al.* (2005a); 3. This paper; 4. Zhesheng *et al.* (1983); 5. Yakubovich *et al*. (2005). For qingheiite, the M(2a)-M(2b) and X(1a)-X(1b) pairs of crystallographic sites have been inverted.

al., 1983; Hatert *et al*., 2005a), but, in ferrowyllieite and in synthetic $Na_{1.265}Mn^{2+}{}_{2.690}Mn^{3+}{}_{0.785}(PO_4)_3$, X(1a) is better described as a distorted cube and X(1b) as a distorted octahedron (Moore & Molin-Case, 1974; Yakubovich *et al*., 2005). This change in topology for the X(1b) site probably results from the splitting of this site from its inversion centre in ferrowyllieite and in the synthetic compound, but not in ferrorosemaryite and rosemaryite (Table 5). It is also noteworthy that the topology of the cubic X(1b) site of rosemaryite is similar to the topology of the X(1) site in the alluaudite structure (Antenucci *et al*., 1995; Hatert *et al*., 2000).

The X(2) site is described by Moore & Molin-Case (1974) as a highly distorted square antiprism with two supplementary very long distances of 3.58 and 3.62 Å, and by Yakubovich *et al.* (2005) as a trigonal prism with one additional oxygen near the side face. As shown in Table 6, the X(2) site in rosemaryite clearly shows a [7+1] coordination, with 7 "short" bonds ranging from 2.485 to 2.819 Å, and one supplementary very long X(2)–O(3a) bond of 3.045 Å. The coordination polyhedra is shown in Fig. 3c, and can be described as a very distorted gable disphenoid, similar to that observed for the A(2)' site in the alluaudite structure (Hatert *et al*., 2000).

As already noted by Hatert *et al*. (2005a) for ferrorosemaryite, the distributions of Fe^{3+} and Al^{3+} between the M(2a) and M(2b) crystallographic sites in rosemaryite and qingheiite are different from that occurring in ferrowyllieite (Table 9). In ferrowyllieite and in synthetic $Na_{1.265}Mn^{2+}{}_{2.690}Mn^{3+}{}_{0.785}(PO_4)_3$, the very large Fe^{2+} and Mn^{2+} cations, with effective ionic radii of 0.780 and 0.830 Å, respectively (Shannon, 1976), preferentially occupy the M(2a) site, while Al^{3+}, with an effective ionic radius of 0.535 Å, preferentially occupies the M(2b) site. In ferrorosemaryite, rosemaryite, and qingheiite, the difference in ionic radii between the cations occupying the M(2a) and M(2b) sites decreases, thus leading to a different cation distribution in which Al^{3+} predominates on the M(2a) site and Fe^{3+} or Mg^{2+}, with effective ionic radii of 0.645 and 0.720 Å, respectively, occupy the M(2b) site (Table 9). The affinity of Fe^{3+} for the M(2b) site also explains the presence of Mn^{3+} on this site in the wyllieite-type compound synthesized by Yakubovich *et al*. (2005), because the 0.645 Å effective ionic radius of Mn^{3+} (Shannon, 1976) is identical to that of Fe^{3+}.

The different cation distributions between the M(2a) and M(2b) sites also slightly affect the X-sites occupancies. As is indicated in Table 9, the X(1a) site predominantly contains Na^{+} in ferrowyllieite and in the synthetic compound, while it contains Mn^{2+} in ferrorosemaryite, rosemaryite, and qingheiite. In contrast, X(1b) is occupied by Na^{+} in ferrorosemaryite, rosemaryite, and qingheiite,

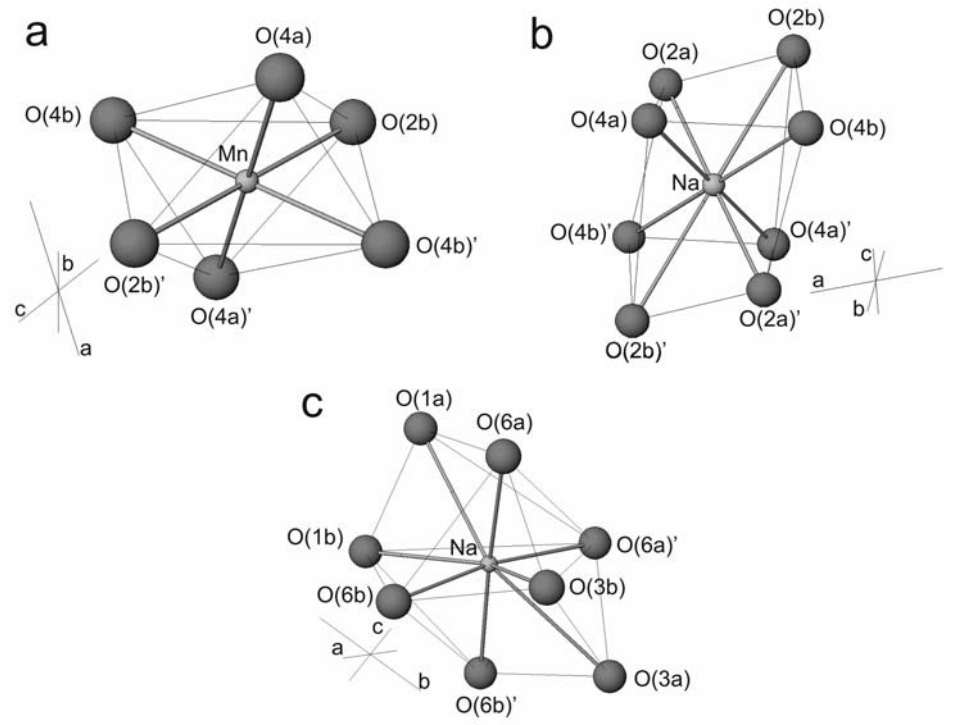

Fig. 3. The X(1a) (a), X(1b) (b) and X(2) (c) crystallographic sites of rosemaryite.

whereas Mn^{2+} and Ca^{2+} occupy the X(1b) site of ferrowyllieite and of the synthetic compound. The X(2) site generally accommodates Na^{+} and vacancies, sometimes with minor amounts of Mn^{2+} or Ca^{2+}.

Mössbauer spectra of wyllieite- and alluaudite-type phosphates

Over the past decade, numerous alluaudite-type phosphates have been synthesized by solid-state reactions or by hydrothermal techniques; see Hatert *et al*. (2000), Hatert (2002), and Hatert (2004) for a recent review of this literature. The synthesis of pure alluaudites has made possible a detailed investigation of the distribution of cations in the alluaudite structure (Antenucci, 1992; Hatert, 2002). In addition, Mössbauer spectral studies of alluaudites (Korzenski *et al*., 1998; Chouaibi *et al*., 2001; Hermann *et al*., 2002; Hatert *et al*., 2003, 2004 and 2005b; Hidouri *et al*., 2004; Redhammer *et al*., 2005) have revealed the existence of next-nearest neighbour interactions between the iron ions found in the octahedral sites of the structure.

The hyperfine parameters obtained for rosemaryite and ferrorosemaryite (Hatert *et al*., 2005a) are similar to those reported for alluaudite-type phosphates. The isomer shifts and quadrupole splittings at 85 K are in the range of 0.51 to 0.55 mm/s and 0.45 to 1.15 mm/s for Fe^{3+} and 1.29 to 1.38 mm/s and 2.30 to 3.25 mm/s for Fe^{2+}, respectively. The iron ions generally occupy the M(2) site, except in ferrorosemaryite, rosemaryite, and the synthetic alluaudite-type $Na_2(Mn_{1-x}Fe^{2+}_x)_2Fe^{3+}(PO_4)_3$ compounds, with x = 0.75 and 1.00, (Hatert *et al*., 2005b), in which iron also occurs at the M(1) site. The 3.13 and 3.284 mm/s quadrupole splittings observed at 85 K for Fe^{2+} on the M(1) site in rosemaryite and ferrorosemaryite are higher than the 3.035 to 3.060 mm/s values observed in synthetic alluaudites, thus indicating that the M(1) site in wyllieites is probably more distorted than in alluaudites.

Finally, it is noteworthy that the Mössbauer spectra of alluaudites and wyllieites are extremely similar and show little significant variation induced by the splitting of the M(2) site into the M(2a) and M(2b) sites. The next-nearest neighbour interactions around the iron ions are similar in these two structure-types, and the use of Mössbauer spectroscopy, which is a local probe, to evaluate the environment of these iron ions, does not reveal any significant differences between these minerals. The ordering of cations, which induces the splitting of the M(2) site into the M(2a) and M(2b) sites on the larger scale of the unit-cell, is within the investigative range of X-ray diffraction but not of Mössbauer spectroscopy.

Stability of wyllieite- and alluaudite-type phosphates, and the role of aluminium

According to Moore & Ito (1973) and Moore & Molin-Case (1974), the occurrence of significant amounts of aluminium in the wyllieite structure, and not in the alluaudites, is responsible for the splitting of the M(2) site. They propose that this splitting occurs because Al^{3+} has a very small effective ionic radius of 0.535 Å (Shannon, 1976), as compared to the 0.780 and 0.645 Å ionic radii of Fe^{2+} and Fe^{3+}, respectively.

Recently, Al-rich phosphates with the nominal $Na_2Mn_2Al(PO_4)_3$ composition have been hydrothermally

synthesized at 300 to 800°C and 1 to 5 kbar (Hatert, 2002). Between 300 and 600°C, white powders without visible crystals were obtained, and the powder X-ray diffraction patterns correspond to those of alluaudite-type phosphates, without any of the supplementary reflections typical of the $P2_1/n$ wyllieite space group. As discussed by Hatert *et al*. (2005a), however, the identification of wyllieite-type phosphates can only be confirmed by single-crystal X-ray diffraction techniques. At 700°C/3.5 kbar and 800°C/1 kbar, tiny acicular crystals were obtained, and single-crystal structure refinements indicated an alluaudite-type structure (Hatert, 2006). Consequently, it appears that the presence of significant amounts of aluminium in the alluaudite structure is not the only parameter which induces the splitting of the M(2) site and the crystallization of wyllieite.

The synthesis of the wyllieite-type phosphate $Na_{1.265}Mn^{2+}_{2.690}Mn^{3+}_{0.785}(PO_4)_3$, at 400°C and 0.1 kbar (Yakubovich *et al*., 2005), force us to conclude that aluminium is not necessary to stabilize the wyllieite structure, and that wyllieite-type phosphates crystallize at lower temperatures than alluaudites. This last result is contradictory to the hypothesis of Moore & Ito (1973) and Moore & Molin-Case (1974), who indicated that ferrowyllieite is of primary origin, whereas alluaudites are secondary.

Because of their highly versatile structure, alluaudite-type phosphates are able to crystallize under various temperature and pressure conditions, and their origin in granitic pegmatites can be primary or secondary (Hatert, 2002, 2004; Fransolet *et al*., 2004). But the ordering responsible for the crystallization of wyllieite-type phosphates seems to occur over a narrow range of temperature and pressure. When cations with very different effective ionic radii occupy the M(2) site, low temperatures can induce the crystallisation of ordered wyllieites, whereas high temperatures induce the disordered cation distribution leading to the crystallisation of alluaudite (Hatert, 2002, 2006). Further experimental investigations, starting from the $Na_2Mn_2Al(PO_4)_3$ composition, are necessary to obtain single-crystal data well below 700°C and to eventually detect the presence of wyllieite-type phosphates.

Acknowledgements: The authors thank Dr. M.-R. Spirlet for help using the four-circle diffractometer, as well as two anonymous reviewers for their constructive comments. F. H. and A. M. F. acknowledge, with thanks, support from the "Fonds National de la Recherche Scientifique," Belgium, for a position of «Chargé de Recherches» and for the grant 1.5.112.02., respectively. F. G. acknowledges, with thanks, support from the "Fonds National de la Recherche Scientifique," Belgium, for the grant 9.4565.95.

References

Antenucci, D. (1992): Synthèse et cristallochimie de composés à structure alluaudite. Incidences dans les processus d'altération des phosphates Fe-Mn des pegmatites granitiques. Unpublished Ph. D. Thesis, University of Liège, 259 p.

Antenucci, D., Miehe, G., Tarte, P., Schmahl, W.W., Fransolet, A.-M. (1993): Combined X-ray Rietveld, infrared and Raman study of a new synthetic variety of alluaudite, $NaCdIn_2(PO_4)_3$. *Eur. J. Mineral.*, **5**, 207-213.

Antenucci, D., Fransolet, A.-M., Miehe, G., Tarte, P. (1995): Synthèse et cristallochimie de $NaCaCdMg_2(PO_4)_3$, phosphate nouveau à structure alluaudite sans cation trivalent. *Eur. J. Mineral.*, **7**, 175-181.

Brier, M. (2000): Röntgenographische Kristallstrukturbestimmung zur Elementverteilung in Mischkristallen der Alluaudit-Wyllieit-Gruppe. Unpublished Diploma thesis, University of Stuttgart, 171 p.

Brown, I.D. & Altermatt, D. (1985): Bond-valence parameters obtained from a systematic analysis of the inorganic crystal structure database. *Acta Cryst.*, **B41**, 244-247.

Černý, P. (1991): Rare-element granitic pegmatites. Part I: Anatomy and internal evolution of pegmatite deposits. *Geosci. Canada*, **18(2)**, 49-67.

Chouaibi, N., Daidouh, A., Pico, C., Santrich, A., Veiga, M.L. (2001): Neutron diffraction, Mössbauer spectrum, and magnetic behavior of $Ag_2FeMn_2(PO_4)_3$ with alluaudite-like structure. *J. Solid State Chem.*, **159**, 46-50.

Dowty, E. (1993): Atoms for Windows. Version 2.3. Shape Software, 521 Hidden Valley Road, Kingsport, TN 37663, USA.

Farmer, V.C. (1974): The infrared spectra of minerals. Mineralogical Society Monographs, **4**, 539 p.

Fransolet, A.-M. (1995): Wyllieite et rosemaryite dans la pegmatite de Buranga, Rwanda. *Eur. J. Mineral.*, **7**, 567-575.

Fransolet, A.-M., Antenucci, D., Fontan, F., Keller, P. (1994): New relevant data on the crystal chemistry, and on the genetical problem of alluaudites and wyllieites. *Abstracts of the 16th IMA general meeting, Pisa*, 125-126.

Fransolet, A.-M., Hatert, F., Fontan, F., (2004): Petrographic evidence for primary hagendorfite in an unusual assemblage of phosphate minerals, Kibingo granitic pegmatite, Rwanda. *Can. Min.*, **42**, 697-704.

Guesmi, A. & Driss, A. (2002): $AgCo_3PO_4(HPO_4)_2$. *Acta Cryst.*, **C58**, i16-i17.

Hatert, F. (2002): Cristallochimie et synthèse hydrothermale d'alluaudites dans le système Na-Mn-Fe-P-O : contribution au problème de la genèse de ces phosphates dans les pegmatites granitiques. Unpublished Ph. D. Thesis, University of Liège, 247 p.

— (2004): Etude cristallochimique et synthèse hydrothermale des alluaudites: contribution nouvelle au problème génétique des phosphates de fer et de manganèse dans les pegmatites granitiques et, partant, à celui de l'évolution de ces gisements. *Mém. Acad. royale Sci. Belgique, Cl. Sci., Coll. in-8°, 3ème série*, **XXI**, 96 p.

— (2006): $Na_{1.50}Mn_{2.48}Al_{0.85}(PO_4)_3$, a new synthetic alluaudite-type compound. *Acta Cryst.*, **C62**, i1-i2.

Hatert, F., Keller, P., Lissner, F., Antenucci, D., Fransolet, A.-M. (2000): First experimental evidence of alluaudite-like phosphates with high Li-content: the $(Na_{1-x}Li_x)MnFe_2(PO_4)_3$ series (x = 0 to 1). *Eur. J. Mineral.*, **12**, 847-857.

Hatert, F., Antenucci, D., Fransolet, A.-M., Liégeois-Duyckaerts, M. (2002): The crystal chemistry of lithium in the alluaudite structure: a study of the $(Na_{1-x}Li_x)CdIn_2(PO_4)_3$ solid solution (x = 0 to 1). *J. Solid State Chem.*, **163**, 194-201.

Hatert, F., Hermann, R.P., Long, G.J., Fransolet, A.-M., Grandjean, F. (2003): An X-ray Rietveld, infrared, and Mössbauer spectral study of the $NaMn(Fe_{1-x}In_x)_2(PO_4)_3$ alluaudite-like solid solution. *Am. Mineral.*, **88**, 211-222.

Hatert, F., Long G.J., Hautot, D., Fransolet, A.-M., Delwiche, J., Hubin-Franskin, M.J., Grandjean, F. (2004): A structural,

magnetic, and Mössbauer spectral study of several Na-Mn-Fe-bearing alluaudites. *Phys. Chem. Mineral.*, **31**, 487-506.

Hatert, F., Lefèvre, P., Fransolet, A.-M., Spirlet, M.-R., Rebbouh, L., Fontan, F., Keller, P. (2005a): Ferrorosemaryite, $NaFe^{2+}Fe^{3+}Al(PO_4)_3$, a new phosphate mineral from the Rubindi pegmatite, Rwanda. *Eur. J. Mineral.*, **17**, 749-759.

Hatert, F., Rebbouh, L., Hermann, R.P., Fransolet, A.-M., Long, G.J., Grandjean, F. (2005b): Crystal chemistry of the hydrothermally synthesized $Na_2(Mn_{1-x}Fe^{2+}_x)_2Fe^{3+}(PO_4)_3$ alluaudite-type solid solution. *Am. Mineral.*, **90**, 653-662.

Hermann, R.P., Hatert, F., Fransolet, A.-M., Long, G.J., Grandjean, F. (2002): Mössbauer spectral evidence for next-nearest neighbor interactions within the alluaudite structure of $Na_{1-x}Li_xMnFe_2(PO_4)_3$. *Solid State Sci.*, **4**, 507-513.

Hidouri, M., Lajmi, B., Wattiaux, A., Fournés, L., Darriet, J., Amara, M. B. (2004): Characterization by X-ray diffraction, magnetic susceptibility and Mössbauer spectroscopy of a new alluaudite-like phosphate: $Na_4CaFe_4(PO_4)_6$. *J. Solid State Chem.*, **177**, 55-60.

Korzenski, M.B., Schimek, G.L., Kolis, J.W., Long, G.J. (1998): Hydrothermal synthesis, structure, and characterization of a mixed-valent iron (II/III) phosphate, $NaFe_{3.67}(PO_4)_3$: a new variation of the alluaudite structure type. *J. Solid State Chem.*, **139**, 152-160.

Leroux, F., Mar, A., Payen, C., Guyomard, D., Verbaere, A., Piffard, Y. (1995a): Synthesis and structure of $NaMn_3(PO_4)(HPO_4)_2$, an unoxidized variant of the alluaudite structure type. *J. Solid State Chem.*, **115**, 240-246.

Leroux, F., Mar, A., Guyomard, D., Piffard, Y. (1995b): Cation substitution in the alluaudite structure type : synthesis and structure of $AgMn_3(PO_4)(HPO_4)_2$. *J. Solid State Chem.*, **117**, 206-212.

Lii, K.-H. & Shih, P.-F. (1994): Hydrothermal synthesis and crystal structures of $NaCo_3(PO_4)(HPO_4)_2$ and $NaCo_3(AsO_4)(HAsO_4)_2$: synthetic modifications of the mineral alluaudite. *Inorg. Chem.*, **33**, 3028-3031.

Moore, P.B. & Ito, J. (1973): Wyllieite, $Na_2Fe^{2+}_2Al(PO_4)_3$, a new species. *Mineral. Rec.*, **4**, 131-136.

—,— (1979): Alluaudites, wyllieites, arrojadites: crystal chemistry and nomenclature. *Min. Mag.*, **43**, 227-235.

Moore, P.B. & Molin-Case, J. (1974): Contribution to pegmatite phosphate giant crystal paragenesis: II. The crystal chemistry of wyllieite, $Na_2Fe^{2+}_2Al(PO_4)_3$, a primary phase. *Am. Mineral.*, **59**, 280-290.

North, A.C.T., Phillips, D.C., Mathews, F.S. (1968): A semi-empirical method of absorption correction. *Acta Cryst.*, **A24**, 351-359.

Redhammer, G., Tippelt, G., Bernroider, M., Lottermoser, W., Amthauer, G., Roth, G. (2005): Hagendorfite $(Na,Ca)MnFe_2(PO_4)_3$ from type locality Hagendorf (Bavaria, Germany): crystal structure determination and ^{57}Fe Mössbauer spectroscopy. *Eur. J. Mineral.*,**17**, 915-932.

Renner, B. & Lehmann, G. (1986): Correlation of angular and bond length distortion in TiO_4 units in crystals. *Z. Kristall.*, **175**, 43.59.

Sarp, H. & Černý, R. (2005): Yazganite, $NaFe^{3+}_2(Mg,Mn)(AsO_4)_3.H_2O$, a new mineral: its description and crystal structure. *Eur. J. Mineral.*, **17**, 367-373.

Shannon, R.D. (1976): Revised effective ionic radii and systematic studies of interatomic distances in halides and chalcogenides. *Acta Cryst*., **A32**, 751-767.

Sheldrick, G.M. (1991): SHELXTL-Plus. Release 4.1. Siemens Analytical X-ray Instruments Inc., Madison, Wisconsin, USA.

— (1997): SHELXS97 and SHELXL97. University of Göttingen, Germany.

Wilson, A.J.C. (1992): International Tables for X-ray Crystallography, Vol. C. Kluwer Academic Press, London, 883 p.

Yakubovich, O.V., Massa, W., Gavrilenko, P.G., Dimitrova, O.V. (2005): The crystal structure of a new synthetic member in the wyllieite group: $Na_{1.265}Mn^{2+}_{2.690}Mn^{3+}_{0.785}(PO_4)_3$. *Eur. J. Mineral.*, **17**, 741-747.

Zhesheng, M., Nicheng, S., Zhizhong, P. (1983): Crystal structure of a new phosphatic mineral-qingheiite. *Sci. Sinica, série B*, **XXVI(8)**, 876-884.

Received 14 March 2006
Modified version received 25 June 2006
Accepted 11 September 2006